Molecular Neurobiology (2019) 56:1707–1718
https://doi.org/10.1007/s12035-018-1164-z

Vdac1 Downregulation Causes Mitochondrial Disintegration Leading to Hippocampal Neurodegeneration in Scopolamine-Induced Amnesic Mice

Meghraj Singh Baghel[1] · Mahendra Kumar Thakur[1]

Received: 27 February 2018 / Accepted: 30 May 2018 / Published online: 19 June 2018

Abstract

Our previous report on hippocampal proteome analysis suggested the involvement of voltage-dependent anion channel (Vdac) 1 in scopolamine-induced amnesia. Further silencing of Vdac1 in young mice reduced the recognition memory. Vdac1 is a porin protein present abundantly on outer mitochondrial membrane. It acts as a transporter of energy metabolites ATP/ADP and Ca^{2+} ions and helps in communication between mitochondrial matrix and cytosol. As Vdac1-associated energy metabolism may be affected during amnesia, we determined the downstream function of Vdac1 in the present study. The expression of Vdac1 and total ATP level was decreased in the hippocampus of scopolamine-induced amnesic mice. Also, the mitochondrial membrane potential, cristae organization, and morphology were disrupted leading to increased ROS generation and reduced SOD and catalase activity. On the other hand, there was increase in the expression of pro-apoptotic marker proteins (Bax, Bad, Casp 3), leading to rising degenerated neuronal cells in the dentate gyrus and Cornu ammonis 3 and 1 subregions of the hippocampus during amnesia. Further, to check whether Vdac1 downregulation is associated with neurodegeneration, we infused Vdac1 siRNA stereotaxically in the hippocampus of normal young mice. As compared to control, Vdac1 silencing decreased ATP level and mitochondrial membrane potential leading to increase in the number of degenerated neuronal cells in subregions of the hippocampus. Taken together, our study shows that downregulation of Vdac1 causes neurodegeneration through mitochondrial disintegration in the hippocampus of scopolamine-induced amnesic mice.

Keywords Scopolamine · Vdac1 · Mitochondria · Apoptosis · Neurodegeneration · Hippocampus

Introduction

Scopolamine, a nonselective antagonist of muscarinic cholinergic receptor, causes memory loss by altering synaptic plasticity associated gene expression [1–3]. It is used widely to generate amnesia in animal models. Using scopolamine-induced amnesic mice, we reported earlier alteration in the protein profile of hippocampus. Among 18 altered proteins, Vdac1 expression was maximally downregulated, showing common interaction with other altered proteins and its silencing in the hippocampus of normal mice impaired recognition memory [4]. Weeber et al. [5] have also shown that Vdac1 deficiency leads to impairment in fear conditioning and spatial memory with disruption in long- and short-term synaptic plasticity in the hippocampus of mice. Vdac1 protein forms a channel in the outer mitochondrial membrane and allows the communication between mitochondrial matrix and cytoplasm, and thus regulates cell metabolism, apoptosis, and reactive oxygen species (ROS) through transportation of ATP/ADP [6]. Vdac1 deficiency reduces the cellular production of ATP in Vdac1 knockout mice [7]. Such failure to produce energy might cause impairment in neural transmission leading to neurodegeneration [8, 9]. Intracerebroventricular injection of amyloid β1–42 peptide causes impairment in learning and memory through depletion of ATP and increase of ROS level leading to Alzheimer's disease (AD) like symptoms in cerebral cortex and hippocampus of mice [10]. Also, exposure to lead

Electronic supplementary material The online version of this article (https://doi.org/10.1007/s12035-018-1164-z) contains supplementary material, which is available to authorized users.

✉ Mahendra Kumar Thakur
mkt_bhu@yahoo.com

[1] Biochemistry and Molecular Biology Laboratory, Department of Zoology, Brain Research Centre, Banaras Hindu University, Varanasi 221005, India

(Pb) and dopamine causes toxicity through downregulation of Vdac1 expression, ATP depletion, ROS elevation, and disruption in mitochondrial membrane potential (MMP) leading to apoptosis during in vitro and in vivo conditions [11, 12]. Also, cannabinoid intoxication induces amnesia through alteration in cellular respiration and energy depletion [13–15]. These studies suggest the involvement of Vdac1 in energy metabolism, cellular function, synaptic transmission, and learning and memory. As Vdac1 was maximally downregulated in the hippocampus of scopolamine-induced amnesic mice, this might be a key regulator of amnesia. Therefore, in the present study, we have explored the downstream function of Vdac1 in scopolamine-induced amnesic mice and reported that its downregulation causes failure of energy production leading to mitochondrial disintegration-mediated hippocampal neurodegeneration.

Experimental Details

Materials

Scopolamine hydrobromide was purchased from Sigma–Aldrich (USA); ENLITEN ATP Assay kit from Promega (USA); carboxy-H2DCFDA from Invitrogen (USA); Rhodamine 123 from Thermo Fisher Scientific (USA), primary antibodies; anti-Vdac1 (ab14734) from Abcam (UK), anti-cytochrome c (sc-13561), anti-Bcl-2 (sc-8392), and anti-caspase 3 (sc-7148) from Santa Cruz Biotechnology (USA); anti-Bax (no. 2772) and Bad (no. 9292) from Cell Signaling Technology (USA); Vdac1 siRNA and negative control siRNA (cat. no. 4390771, 4390843) from Ambion (USA). All other biochemicals were purchased from Merck (Germany).

Animals and Drug Administration

Swiss albino young (10 ± 2 weeks) male mice were inbred and maintained at 24 ± 2 °C under 12 h light and dark cycle with ad libitum access to standard mice feed and drinking water in the animal house of Department of Zoology, Banaras Hindu University, India. They were handled as per guidelines of the Animal Ethical Committee, Banaras Hindu University. Scopolamine hydrobromide (SC) (3 mg/kg body weight) was administered intraperitoneally to experimental mice and saline (SA) (0.9% NaCl) as a vehicle to control mice between 9 and 10 am daily for 7 days. After treatment, control ($n = 20$) and treated ($n = 20$) mouse groups were sacrificed by cervical dislocation, brain was dissected out from the skull, and both cerebral hemispheres were separated in saline. Then, the hippocampi were removed for further experiments [16].

Biochemical Analysis

Analysis of Vdac1 and ATP Level

Protein extract was prepared by homogenizing hippocampus (10%) in RIPA buffer (50 mM TrisCl, pH 7.4, 150 mM NaCl, 0.1% Triton X-100, 0.1% SDS, 2 mM EDTA, 10 mM sodium deoxycholate, and 0.1 mM PMSF) followed by centrifugation at 12,000×*g* for 20 min at 4 °C. The supernatant was collected in a microfuge tube and protein concentration was determined [17]. Equal amount of protein was separated by 10% SDS-PAGE (15% for cytochrome c), blotted to polyvinylidene difluoride (PVDF) membrane (Millipore) and blocked with 5% (*w*/*v*) nonfat skimmed milk for 2–3 h. After blocking, the blots were probed with primary antibody anti-Vdac1. After incubation, the blot was washed in phosphate-buffered saline (PBS) thrice and incubated with HRP-conjugated secondary antibody (1:2000) (Bangalore Genei, India) for 3 h. Then, the blot was washed in PBS and signal was detected using ECL reagents on X-ray film. The same blot was probed with anti-β-actin HRP conjugated antibody (1:20,000) for 4–6 h and used for normalization.

To measure the energy level, ATP was extracted from the tissue using trichloroacetic acid (TCA) as previously described [18] and protocol supplied by the manufacturer with slight modification. The isolated hippocampus was immediately homogenized in 500 μl ice-cold homogenization buffer (0.25 M sucrose and 10 mM HEPES–NaOH, pH 7.4) for three cycles of 30 s each followed by centrifugation at 1000×*g* for 10 min at 4 °C. The supernatant (300 μl) was quickly added to an equal volume of ice-cold 10% TCA, shaken for 20 s, and centrifuged at 10,000×*g* for 10 min at 4 °C. Further, 400 μl of supernatant was transferred to a fresh tube and 200 μl 1 M Tris-acetate buffer (pH 7.75) was added for neutralization. The sample was diluted 30 times with ATP free water and ATP level was measured by luciferase assay through detection of bioluminescence emission. The tissue extract (10 μl) was mixed with 90 μl of luciferase reagent and luminescence was recorded immediately using multimode reader with bioluminescence detector (BioTek SYNERGY H1, USA). For normalization, readings were divided by tissue weight for respective control and experimental groups. Luciferase enzyme utilizes ATP and catalyzes the reaction to release energy in the form of bioluminescence. If high amount of ATP is available for luciferase reaction, it catalyzes more reaction and releases more bioluminescence ($ATP + Luciferin + O_2 \rightarrow Oxyluciferin + AMP + PPi + CO_2 + Light\ 560\ nm$).

Analysis of Mitochondrial Membrane Potential, Ultrastructure, and Calcium Level

To measure the mitochondrial membrane potential, we used Rhodamine 123 (Rh 123) which is a cell-permeant, green fluorescent, cationic dye and accumulates in active

mitochondria. The active mitochondria having normal membrane potential sequesters more amount of Rh 123 and proportionally gives more fluorescent intensity. Mitochondria were isolated from the hippocampus as described earlier with slight changes [19]. The tissue was minced on ice and homogenized in isolation buffer (225 mM mannitol, 75 mM sucrose, 5 mM HEPES, 1 mM EGTA, 1 mg/ml BSA, pH 7.4). The homogenate was centrifuged at 600×*g* for 5 min at 4 °C. The supernatant was collected and centrifuged at 9000×*g* for 8 min at 4 °C. The pellet obtained was resuspended in isolation buffer containing 0.02% heparin and centrifuged at 9000×*g* for 8 min at 4 °C. Finally, the brownish pellet was resuspended in isolation buffer and centrifuged at 9000×*g* for 10 min at 4 °C. The pellet was again suspended in the isolation buffer containing heparin and protein was estimated. Equal amount of mitochondria was taken and incubated with Rh 123 (0.3 μM) dye for 20 min at 37 °C followed by centrifugation at 9000×*g* for 5 min to remove extra dye. Then, fluorescence was recorded in the multimode reader with fluorescence detector at 535 nm (excitation) and 580 nm (emission) wavelength. The fluorescence intensity value was used to reflect the mitochondrial membrane potential.

For mitochondrial ultrastructure, control and treated mouse groups were sacrificed and hippocampus was isolated. It was cut into 2-mm^2 sizes and fixed overnight at 4 °C with Karnovsky fixative containing 2.5% glutaraldehyde and 4% paraformaldehyde in 0.1 M phosphate buffer (pH 7.4). The tissue pieces were washed thrice for 15 min each with 0.1 M phosphate buffer at 4 °C and cut into 1-mm^2 size followed by post-fixation with 1% osmium tetroxide for 2 h at 4 °C. The tissue pieces were dehydrated in ice-cold acetone at 4 °C, cleared with toluene, and embedded in Araldite CY 212. Ultrathin sections (~ 60–90 nm) were cut by ultramicrotome, collected on copper grids, and stained with uranyl acetate and lead citrate. The grids were washed with distilled water and viewed using a transmission electron microscope (FEI Tecnai S Twin at All India Institute of Medical Sciences, New Delhi) at × 5000 magnification for visualization of mitochondrial ultrastructure in the hippocampus as described earlier with slight modification [20].

To measure calcium level, first, mitochondria were isolated and atomic absorption flame spectroscopy (AAS) was performed as described earlier [21]. Hippocampus (60 mg) was cut into small pieces in ice-cold medium (250 mM sucrose, 2 mM HEPES, and 3 μM ruthenium red, pH 7.4). Once rinsed in buffer, tissue was homogenized in 2 ml buffer using homogenizer at speed of 5000 rpm with 5–7 strokes up and down. The homogenate was differentially centrifuged at 1000×*g* for 10 min, and then supernatant was further centrifuged at 10,000×*g* for 14 min to settle down the mitochondria. The pellet was washed once with buffer (equal volume to supernatant) and centrifuged at 10,000×*g* for 14 min. Finally, mitochondrial pellet was resuspended in 1.5 ml buffer and Janus Green staining was used to check the mitochondria. Protein was estimated using Bradford method and equal amount of protein (0.15 mg) was taken to determine the calcium level by using AAS-containing cathode lamp. Samples were prepared through base digestion method with 1 N NaoH and heated at 75 °C in water bath for 15 min twice. After digestion, samples were passed through sterile 0.2-μM syringe filter and used for analysis. The calcium standard curve was developed using different concentrations (1, 4.5, 10 mg/l) by AAS (Perkin Elmer) in the Department of Botany, Banaras Hindu University, as described earlier [22]. Samples were analyzed and readings were noted to calculate the calcium level in micromolars per milligram of protein.

Analysis of ROS and Antioxidant Enzyme Activity

To determine total ROS level, 10% hippocampal homogenate was prepared in PBS followed by centrifugation at 10,000×*g* at 4 °C as described previously [23]. The supernatant was used for protein estimation; equal amount of protein was taken from control and treated samples, and incubated with 2 mM 2′, 7′-dichlorofluorescein diacetate (H2DCFDA) in PBS at 37 °C for 30 min. The available ROS converted nonfluorescent H2DCFDA to highly fluorescent 2′, 7′-dichlorofluorescein (DCF) which was recorded at 488 nm (excitation) and 525 nm (emission) using a multimode reader. The level of ROS in each sample was determined by calculating fluorescence intensity value per milligram of protein.

The antioxidant enzymes catalase and superoxide dismutase (SOD) play a role in defense mechanism of the cell. So, their activity was measured in mouse hippocampus as described earlier with slight modification [24]. Catalase activity was analyzed by native polyacrylamide gel electrophoresis followed by ferricyanide staining method. The homogenate (10%) was prepared in 0.2 mM Tris-HCl (pH 7.4) and centrifuged at 10,000×*g* for 10 min at 4 °C. The supernatant was used for protein estimation and an equal amount of protein was resolved by 8% native PAGE at 4 °C. After completion of electrophoresis, the gel was washed with distilled water and soaked in H_2O_2 (0.003%) for 5–10 min followed by rinsing with distilled water to remove excess H_2O_2. The gel was then stained in a solution containing 1% ferric chloride and 1% potassium ferricyanide for 4–5 min. Thereafter, the achromatic bands appeared and the image was captured by Alpha Innotech gel documentation system for densitometric analysis. For analysis of SOD activity, an equal amount of protein was separated by 10% native PAGE at 4 °C and the gel was soaked in 1.23 mM nitro blue tetrazolium chloride (NBT) solution for 20 min in dark. Then, the gel was washed with distilled water and incubated in 100 mM phosphate buffer (pH 7.0) containing 28 mM TEMED and 0.28 mM riboflavin for 15–20 min in dark. Finally, the gel was exposed to light until achromatic bands appeared with the purple-blue

background; the image was captured and analyzed by Alpha Innotech gel documentation system.

Analysis of Apoptotic Marker Protein Level

To check apoptosis, we have analyzed the level of apoptotic marker proteins in the hippocampus by western blotting as mentioned in the previous section. Equal amount of protein was resolved by 10% SDS-PAGE and blotted to PVDF membrane. For cytochrome c, we isolated the cytosolic and mitochondrial fraction as described earlier [25] and equal amount of cytosolic and mitochondrial fraction protein was separated by 15% SDS-PAGE and blotted to PVDF membrane. Blots were blocked for 2–3 h and probed with primary antibodies anti-cytochrome c (1:500), anti-Bax (1:1000), anti-Bad (1:1000), caspase 3 (1:1000), and anti-Bcl-2 (1:500) diluted in blocking buffer overnight at 4 °C. After incubation, the blots were washed in PBS thrice and incubated with HRP-conjugated secondary antibodies (1:2000) for 3 h. Then, the blots were washed in PBS and signal was detected on X-ray film. The same blot was probed with anti-β-actin HRP-conjugated antibody for 4–6 h and used for normalization.

Analysis of Neurodegeneration

For detection of degenerated neurons in the hippocampus of control and treated mice, the brain was processed as described earlier. The tissue was first fixed in 4% paraformaldehyde (PFA) overnight, then immersed in 30% sucrose and finally embedded in optimum cutting temperature (OCT) solution. Transverse 8-μm thick sections were cut by a cryostat (Leica Biosystem, Germany), mounted on poly-L-lysine-coated slides and stored at − 80 °C for FJC staining. FJC dye is a polyanionic fluorescein-derived molecule which selectively binds to degenerated neurons and is used to detect neurodegeneration [26]. To visualize degenerated neuronal cells, the brain sections were immersed in a solution of 1% NaOH for 5 min, followed by rinsing with 70% ethanol and distilled water for 2 min each [27]. Then, sections were incubated in 0.06% potassium permanganate solution for 10 min and rinsed in distilled water for 2 min. Further, slides were incubated in FJC staining solution (stock solution 0.01% in water; diluted in 0.1% acetic acid) for 25 min. Then, slides were washed for 1 min thrice and air-dried at 50 °C for 30 min. After clearing in xylene, sections were mounted with DPX solution and a coverslip was applied. Slides were observed and hippocampal subregions dentate gyrus (DG) and Cornu ammonis (CA) 3 and CA1 were focused under the fluorescence microscope (Leica, Germany) with FITC filter. The images were captured at × 40 resolution and FJC-positive cells were counted using ImageJ software (NIH, USA).

Intrahippocampal Vdac1 siRNA Infusion

To silence Vdac1 expression, Vdac1 siRNA and nontargeting sequence as a negative control (NC) were infused bilaterally into the hippocampus stereotaxically as described earlier [4]. The mice were anesthetized by administration of sodium pentobarbital (40 mg/kg bw i.p.). Hair was removed from the head and fixed on stereotaxic stage. Initially, coordinates (2 mm frontal to lambda, 2 mm lateral to midline, and 1.4 mm depth from the skull surface) were set to hippocampus and slowly a hole was made by additional needle. The Vdac1 siRNA sequence (sense 5′-GUCAGAGAAUGGAUUGGAAtt-3′, antisense 5′-UUCCAAUCCAUUCUCUGACtt-3′) was validated through siRNA-Check online bioinformatics tool (http://projects.insilico.us/SpliceCenter/siRNACheck). Vdac1 siRNA (3 μg/5 μl) and NC was infused at the rate of 1 μl/min. After infusion, the animal was removed from the apparatus and incision was stitched and nebasulf powder was employed for normal recovery. All the animals were kept in separate cages and exposed to table lamp for warming. After 5 days of the recovery, mice were sacrificed and the hippocampus was separated. The expression of Vdac1 protein was analyzed by western blotting, ATP level by luciferase assay, MMP by Rh 123 dye, and neurodegeneration by FJC staining as described in previous sections.

Statistical Analysis

The data of control and experimental groups obtained from western blotting, ATP assay, ROS level, the density value of achromatic band of antioxidant enzymes activity, the fluorescence intensity of Rh123, and FJC-positive cell number were analyzed and values were presented as the mean ± SEM. Student's t test was used to determine statistical significance by SPSS 16.0 (Statistical Products and Service Solutions, IBM Corporation, Armonk, NY, USA). The p value < 0.05 was considered as statistically significant.

Results

Effect of Scopolamine on Vdac1 and ATP Level

The level of Vdac1 protein was downregulated (45%) and ATP level was reduced (55%) in the hippocampus of scopolamine-induced amnesic mice as compared to control (Fig. 1). Such depletion in ATP level might occur through Vdac1 downregulation.

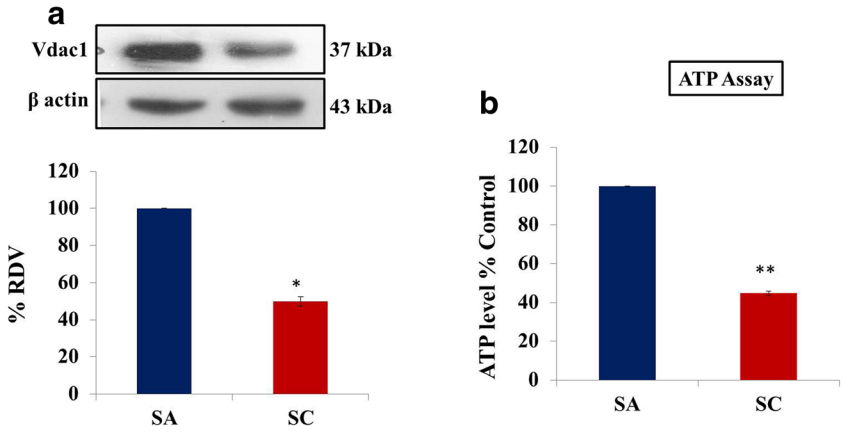

Fig. 1 Effect of scopolamine on Vdac1 and ATP level. **a** Western blot analysis of Vdac1expression. Histogram represents relative density value (RDV) (Vdac1a/ß actin). **b** Luciferase assay analysis to measure ATP level. Histogram shows bioluminescence intensity-based % ATP level. Data are represented as mean ± SEM of three animals in each group. Statistically significant difference is represented as one ($p < 0.01$) and two ($p < 0.001$) asterisks in scopolamine (SC) group as compared to saline control (SA)

Effect of Scopolamine on Mitochondrial Membrane Potential, Ultrastructure, and ATP Level

As reduced ATP level affects mitochondrial integrity, we checked it and analyzed mitochondrial membrane potential using Rh 123 dye. Both mitochondrial membrane potential and accumulation of Rh 123 in mitochondria declined significantly, suggesting disruption of mitochondrial membrane potential in the hippocampus of scopolamine-induced amnesic mice as compared to control (Fig. 2a).

In electron micrograph, we observed that mitochondria were small in size, more spherical in shape, and have damaged

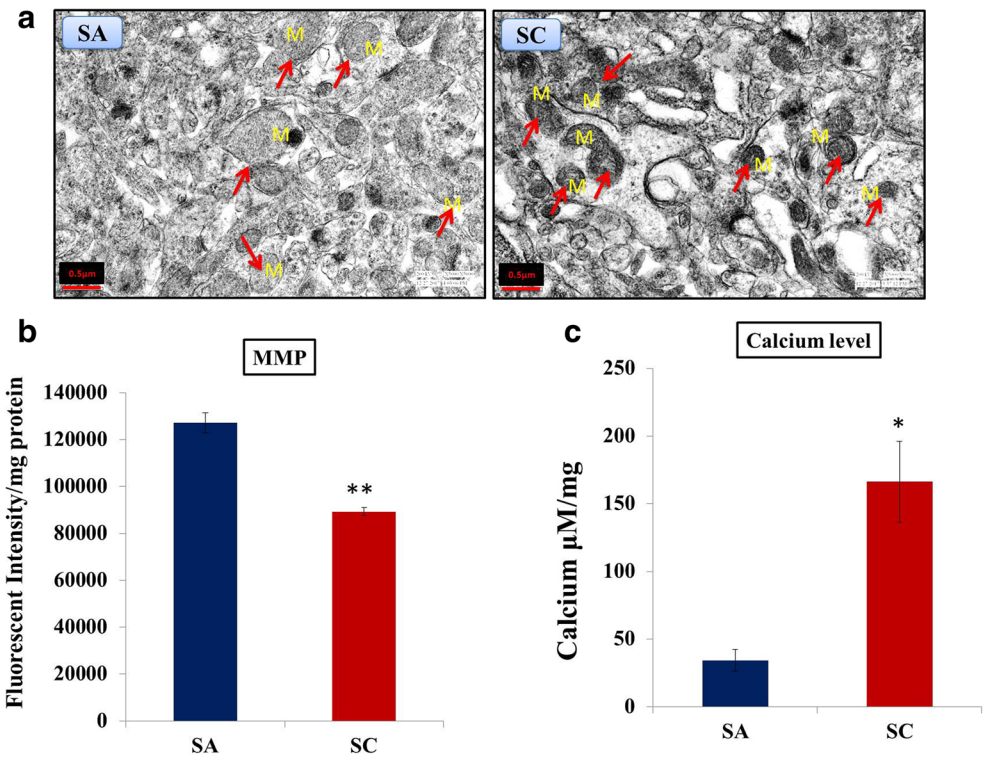

Fig. 2 Effect of scopolamine on mitochondrial ultrastructure, membrane potential, and calcium level. **a** Electron micrograph revealed small size, more spherical shape, and damaged cristae in mitochondria of scopolamine-induced amnesic mice. Mitochondria appeared blackish in amnesic mice. M, mitochondria. Arrows indicate mitochondria. Scale bar, 0.5 μm. **b** Analysis of mitochondrial membrane potential: histogram shows comparative fluorescent intensity values. **c** Measurement of calcium level in mitochondria: histogram shows calcium level in isolated mitochondria. Values are represented as mean + SEM of three animals in each group. Statistically significant difference is represented as one ($p < 0.05$) and two ($p < 0.01$) asterisks in SC group as compared to SA

cristae in the hippocampus of scopolamine-induced amnesic mice. Mitochondria appeared blackish in the hippocampus of amnesic mice, but they were small and elongated with clearly visible larger cristae in control. The blackish appearance of mitochondria could be due to the deposition of calcium ions during apoptosis (Fig. 2b). To confirm this, we analyzed the calcium level in mitochondria of control and scopolamine-induced amnesic hippocampus. Interestingly, we observed that calcium level was very high in mitochondria of scopolamine-induced amnesic hippocampus as compared to control (Fig. 2c). This indicates that the blackish appearance of mitochondria might be due to accumulation of calcium.

Effect of Scopolamine on ROS Level and Antioxidant Enzyme Activity

As reduced ATP level in the hippocampus of amnesic mice might affect the normal mitochondrial function and disrupt the cell homeostasis, we checked ROS level and the activity of its scavenging enzymes (SOD and catalase). ROS level (fluorescent intensity) was increased (Fig. 3a), and the activity of antioxidant enzymes SOD (35.47%) and catalase (42.47%) decreased in the hippocampus of scopolamine-induced amnesic mice as compared to control (Fig. 3b).

Effect of Scopolamine on Apoptotic Marker Protein Level

As alteration in the mitochondrial integrity during amnesia might trigger the intrinsic pathway of apoptosis, we analyzed the level of cytosolic cytochrome c, Bax, Bad, Bcl-2, and caspase 3 protein. The level of cytosolic cytochrome c and pro-apoptotic proteins (Bax, Bad, Pro-Caspase 3) increased but the level of the cyt c in mitochondrial fraction (Supplementary Fig. 2) and anti-apoptotic protein (Bcl-2) decreased in the hippocampus of scopolamine-induced amnesic mice as compared to control (Fig. 4).

Effect of Scopolamine on Neurodegeneration

As elevated expression of apoptotic proteins is a sign of apoptosis and cell death, we analyzed neurodegeneration during scopolamine-induced amnesia. Through microscopic visualization of FJC staining, we observed significantly high number of degenerated FJC positive neuronal cells in DG, CA3, and CA1 subregions of the hippocampus of scopolamine-induced amnesic mice as compared to control. This indicated relatively higher neurodegeneration in the hippocampus of amnesic mice (Fig. 5).

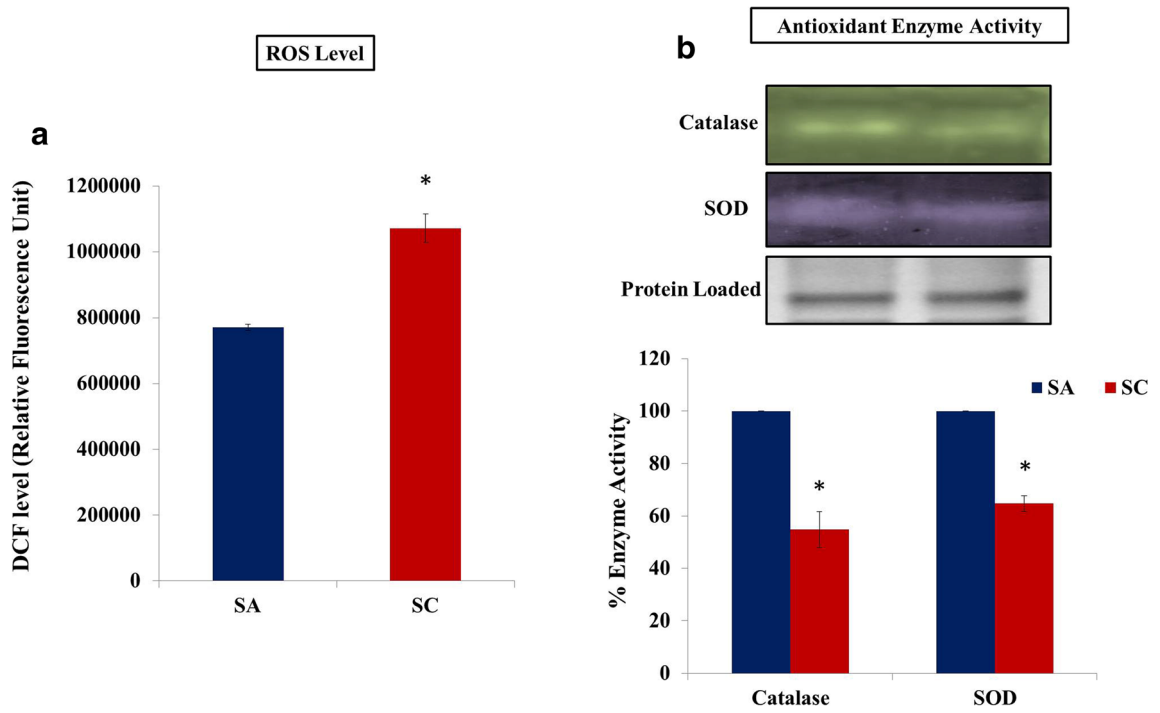

Fig. 3 Effect of scopolamine on ROS and antioxidant enzyme activity. **a** Measurement of ROS level: histogram shows DCF fluorescence intensity values. **b** Activity of antioxidant enzymes (SOD and catalase) was analyzed in the hippocampus of amnesic mice and density values are plotted. Data are represented as mean ± SEM of three animals in each group. Statistically significant difference is represented as one asterisk ($p < 0.05$) in SC group as compared to SA

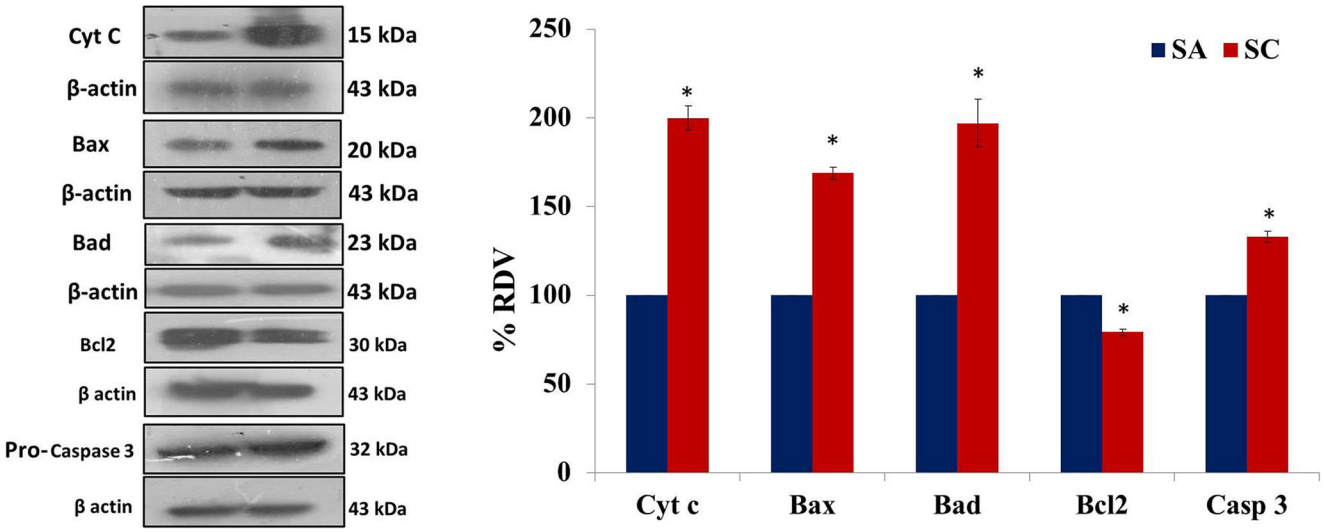

Fig. 4 Effect of scopolamine on apoptotic marker protein level: Western blot analysis of pro-apoptotic and anti-apoptosis proteins. Histogram represents relative density value (RDV) (cyt c, Bax, Bad, Casp3, Bc1–2/ß actin). Data are represented as mean ± SEM of three animals in each group. Statistically significant difference is represented as one ($p < 0.05$) and two ($p < 0.01$) asterisks in SC group as compared to SA

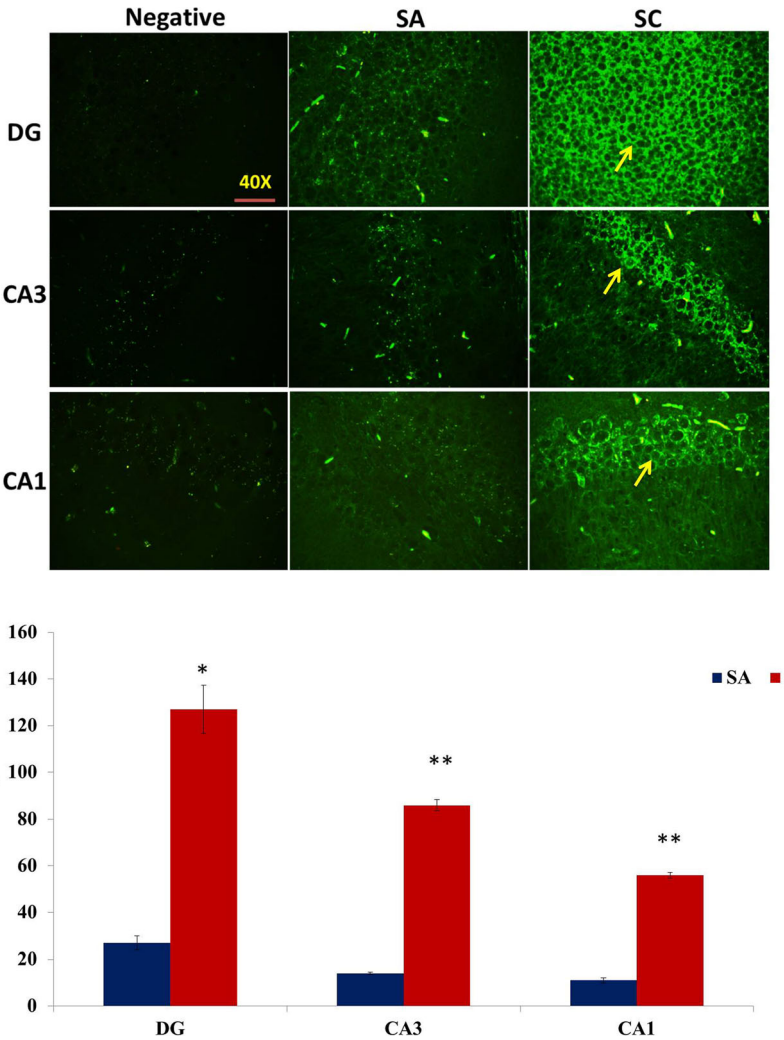

Fig. 5 Effect of scopolamine on neurodegeneration: The panels show representative images of Fluro-Jade C staining in DG, CA3, and CA1 subregions of hippocampal neurons. Graph represents increased number of Fluro-Jade C-positive degenerated neuronal cells in the hippocampal subregions of scopolamine-induced amnesic mice. Arrows indicate FJC-positive cells. Data are represented as mean ± SEM of three animals in each group. Statistically significant difference is represented as one ($p < 0.01$) and two ($p < 0.001$) asterisks in SC group as compared to SA

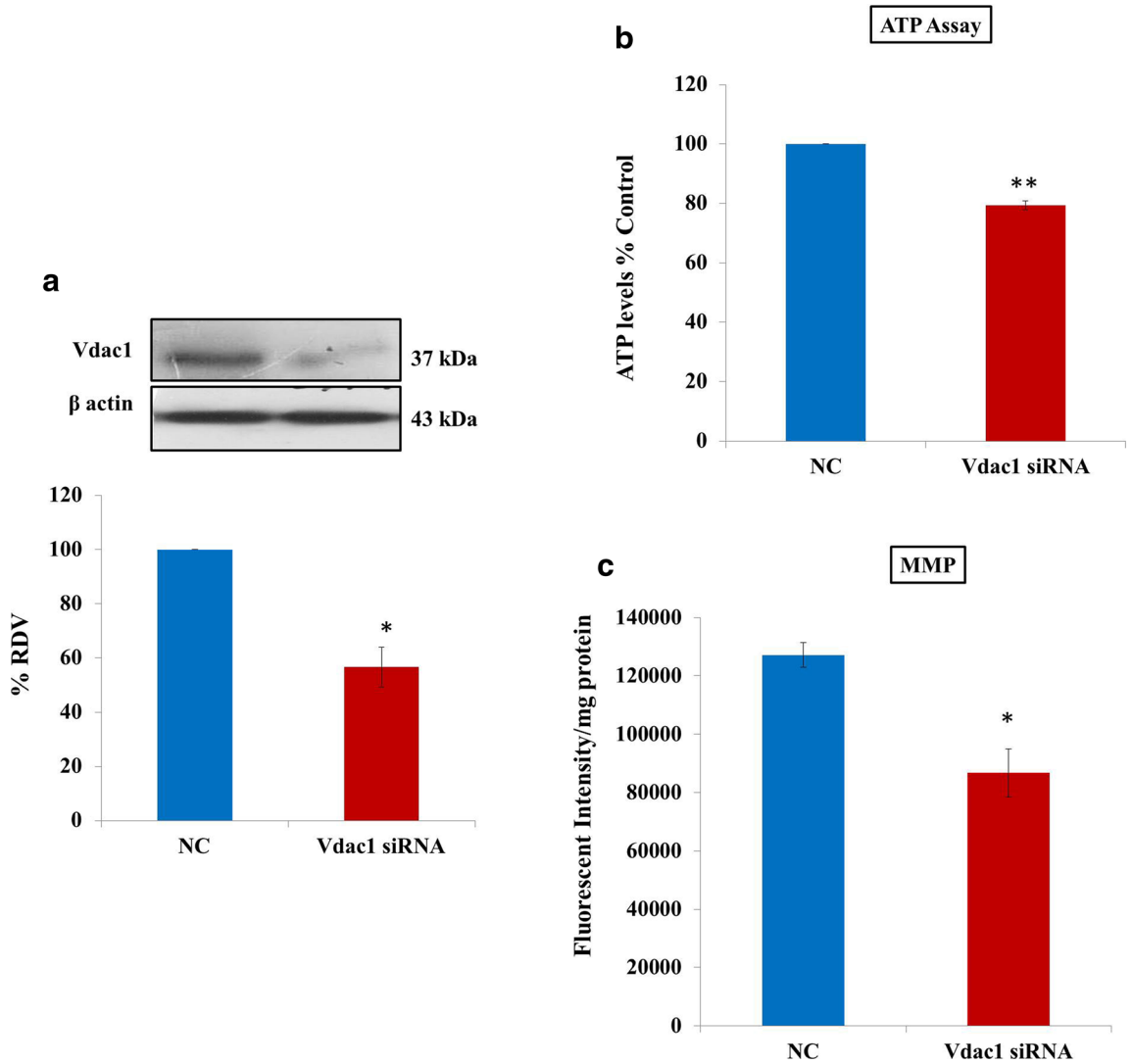

Fig. 6 Effect of Vdac1 silencing on Vdac1, ATP level, and mitochondrial membrane potential. **a** Western blot analysis of Vdac1protein: histogram represents relative density value (RDV) (Vdac1/ß actin). **b** Luciferase assay to measure ATP level: histogram shows bioluminescence intensity-based % ATP level. **c** Analysis of mitochondrial membrane potential: histogram shows fluorescent intensity values. Data are represented as mean ± SEM of three animals in each group. Statistically significant difference is represented as one ($p < 0.01$) and two ($p < 0.001$) asterisks in Vdac1 siRNA group as compared to negative control (NC)

Effect of Vdac1 Silencing on Vdac1, ATP, MMP, and Neurodegeneration

As the downstream function of Vdac1 is affected in scopolamine-induced amnesia, we checked whether downregulation of Vdac1 increased neurodegeneration. Therefore, we planned to silence Vdac1 protein in the hippocampus of normal young mice. The level of Vdac1 protein and total ATP decreased significantly in siRNA-infused hippocampus as compared to NC (Fig. 6a). Also, mitochondrial membrane integrity was altered and mitochondrial membrane potential was decreased in Vdac1-silenced mice as compared to control (Fig. 6c). Further, we found that Vdac1 silencing significantly increased the degenerated FJC-positive neuronal cells in DG, CA3, and CA1 subregions of the hippocampus of mice as compared to NC (Fig. 7). These results suggested that downregulation of Vdac1 might cause depletion of ATP, mitochondrial disintegration, and increase in the number of degenerated neuronal cells in the hippocampus of scopolamine induced-amnesic and Vdac1-silenced mice.

Discussion

Earlier, we reported that the level of 18 proteins was altered in the hippocampus of scopolamine-induced amnesic mice. Among these proteins, Vdac1 level was maximally downregulated and showed common interaction with other altered proteins as assessed by in silico analysis. Moreover, silencing of Vdac1 in the hippocampus of normal young mice showed

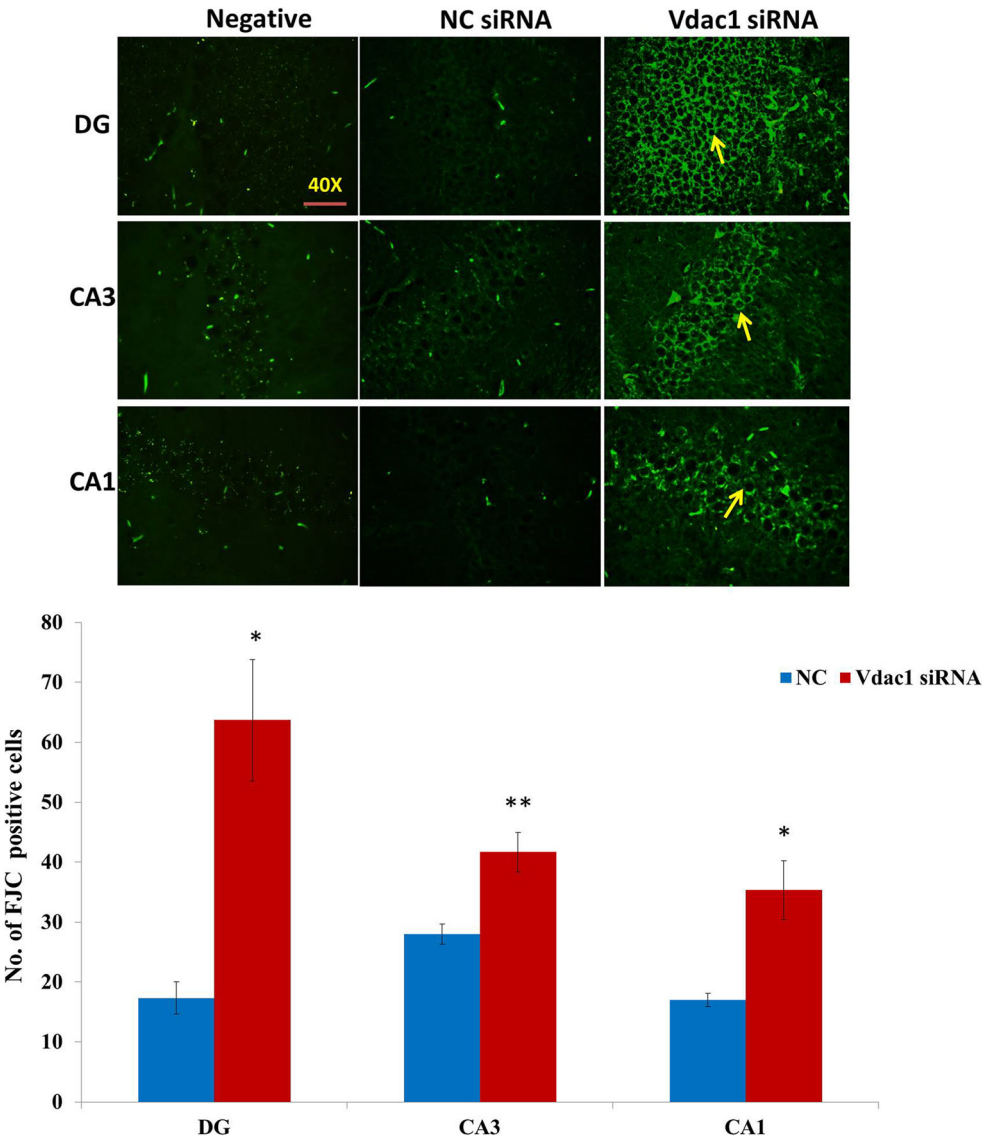

Fig. 7 Effect of Vdac1 silencing on neurodegeneration: The panels show representative picture of Fluro-Jade C staining in DG, CA3, and CA1 subregions of hippocampus. Histogram represents increased number of FJC-positive neuronal cells in the hippocampal subregions of Vdac1-silenced mice. Arrows indicate FJC-positive cells. Data are presented as mean ± SEM of three animals in each group. Statistically significant difference is represented as one ($p < 0.05$) and two ($p < 0.01$) asterisks in Vdac1 siRNA group as compared to NC

impairment in recognition memory. These findings suggested that downregulation of Vdac1 in the hippocampus might be involved in memory impairment during scopolamine-induced amnesia and Vdac1 silencing in mice. Vdac1 is an energy transporter protein present on outer mitochondrial membrane. So, its downregulation might be affecting its associated function in the hippocampus leading to memory impairment. Therefore, in the present study, we explored Vdac1 downstream function during scopolamine-induced amnesia.

As we observed downregulation of Vdac1, this might impair ATP/ADP transportation leading to depletion of ATP level in the hippocampus of scopolamine-induced amnesic mice. Earlier, it has been reported that cannabinoid induces memory loss by impairing the mitochondrial function and energy metabolism [12]. Reduced ATP level is detrimental to the cellular homeostasis and might trigger oxidative damage, disruption of mitochondrial membrane potential, and ultrastructure leading to apoptosis during amnesia [28]. It has been elucidated that oxidation of metabolites and production of ATP level are altered in Vdac1-deficient animals [29] and cause defects in energy production pathway and structural and functional integrity of mitochondria [30, 31]. A recent study showed that metformin, which is used as a drug to reduce glucose level in type 2 diabetic patients, acts as energy disruptor and causes loss of mitochondrial integrity through disorganization of cristae [32]. We noted decreased mitochondrial membrane potential, disorganized cristae, and increased small mitochondria in the hippocampus of scopolamine-induced amnesic mice. Such damage to cristae, disruption of membrane potential, and more defective small size mitochondria might cause apoptosis and neurodegeneration [33]. It has been suggested that deregulation of fission, a process of mitochondrial dynamics, takes place by which small-sized mitochondria are accumulated during the apoptotic process [34]. In addition, we also observed very high calcium levels in

mitochondria of scopolamine-induced amnesic mice. This accumulation of calcium in the mitochondria might cause blackish appearance as observed in transmission electron micrograph of scopolamine-induced amnesic mice. An earlier report has shown that calcium precipitates with phosphate and sequesters in the form of granules which give blackish appearance to mitochondria [35, 36]. Accumulation of calcium in the mitochondria induces cytochrome c release and triggers apoptosis [37].

As mitochondria are the major source of ROS, defects in mitochondria raise ROS level, release of cytochrome c to cytosol, and reduction of antioxidant enzyme activity, leading to mitochondria-mediated apoptosis during aging and neurodegenerative diseases [38–40]. Similarly, we also found increased ROS generation and reduced antioxidant enzyme activity in the hippocampus of amnesic mice. These results suggest that depletion of ATP, elevation of ROS level, and reduction of antioxidant enzyme activity might trigger mitochondria-mediated apoptosis leading to neurodegeneration in the hippocampus of amnesic mice.

Therefore, in the later part of the study, we checked the molecular markers of apoptosis. We found that the cytosolic cytochrome c level was increased, pro-apoptotic proteins (Bax, Bad, caspase 3) were upregulated, and anti-apoptotic protein Bcl-2 was downregulated in the hippocampus of scopolamine-induced amnesic mice. Interaction of Bcl-2 with Vdac1 regulates mitochondrial pore complex and membrane potential, thus preventing the release of cytochrome c and apoptosis [41–43]. Our study suggests that downregulation of Vdac1 and Bcl-2 might affect their interaction to prevent apoptosis and might help in apoptosis. Moreover, loss of mitochondrial membrane potential causes pore formation and increases release of cytochrome c leading to apoptosis. Cytochrome c further forms apoptosome and activates the caspases which lead to DNA fragmentation and apoptosis, resulting in neurodegeneration. In addition, scopolamine-induced apoptosis also increased the FJC-positive degenerated neuronal cells in DG, CA3, and CA1 subregions of the hippocampus of amnesic mice and thus increased neurodegeneration. An earlier report has also demonstrated that dopamine administration causes disruption in mitochondrial membrane potential through downregulation of Vdac1 and subsequently neurodegeneration in human neuroblastoma cells. However, overexpression of Vdac1 is rescued from the toxic effect of dopamine [15]. These experimental evidences suggest that downregulation of Vdac1-mediated mitochondrial disintegration causes apoptosis and neurodegeneration in the hippocampus of scopolamine-induced amnesic mice.

Further, to check whether Vdac1 downregulation is involved in neurodegeneration during scopolamine-induced amnesia, we silenced Vdac1 expression in the hippocampus of normal young mice and observed reduction in total ATP level, mitochondrial membrane potential, and increased FJC-positive degenerated neuronal cells in the hippocampal subregions. Loss of membrane potential of mitochondria leads to

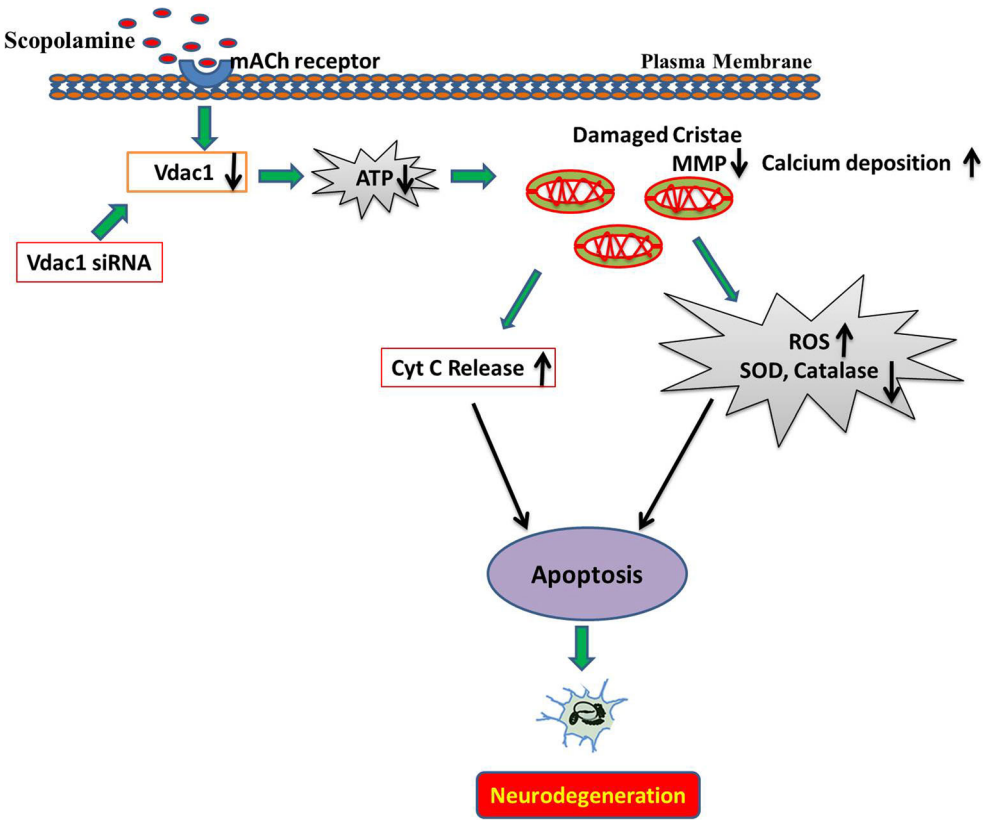

Fig. 8 Proposed mechanism for altered energy metabolic pathway in the hippocampus of scopolamine-induced amnesic mice: Vdac1 downregulation causes depletion of ATP level, mitochondrial disintegration, ROS elevation, and reduction in antioxidant enzyme activity leading to apoptosis and neurodegeneration in the hippocampus of scopolamine-induced amnesic and Vdac1-silenced mice

disintegration which subsequently triggers molecular events of apoptosis. Earlier, Arif et al. [44] have demonstrated that Vdac1 silencing in different cancer cell lines inhibits cell growth through decrease in the mitochondrial membrane potential and ATP level. Deregulation of Vdac-mediated mitochondrial dysfunction is also associated with neurodegenerative diseases and cancer [45]. However, our findings suggest that downregulation of Vdac1 leads to depletion of ATP, mitochondrial disintegration, apoptosis, and neurodegeneration in the hippocampus of scopolamine-induced amnesic mice. In addition, hippocampal Vdac1-silencing also showed ATP depletion, mitochondrial disintegration, and neurodegeneration leading to impairment in recognition memory of normal young mice similar to scopolamine treatment.

Taken together, our present and previous findings show that downregulation of the energy transporter protein Vdac1 and impairment of its downstream function resulted in the depletion of ATP level, mitochondrial disintegration, and increased number of degenerated neuronal cells in the hippocampus of scopolamine-induced amnesic mice. Further, hippocampal Vdac1-silencing in normal young mice showed reduction in ATP level and mitochondrial membrane potential, which in turn increased the number of degenerated neuronal cells. Thus, our findings suggest that downregulation of Vdac1 is associated with ATP depletion and mitochondrial disintegration leading to neurodegeneration in the hippocampus of scopolamine-induced amnesic and Vdac1-silenced mice as presented in Fig. 8. Further studies are warranted to elucidate energy-dependent calcium transport in mitochondria during scopolamine-induced amnesia. This will establish the role of mitochondria in hippocampal neurodegeneration and help in understanding the mechanism of energy impairment in neurodegenerative diseases.

Acknowledgements Meghraj Singh Baghel thanks University Grants Commission-Centre for Advanced Study, Department of Zoology, for the award of Senior Research Fellowship. We thank Prof. TC Nag, All India Institute of Medical Sciences, New Delhi, for discussing the TEM results.

Funding information Financial support from the Department of Biotechnology, Department of Science and Technology, and Indian Council of Medical Research, Government of India, are highly acknowledged.

Compliance with Ethical Standards

Conflict of Interest The authors declare that they have no conflict of interest.

References

1. Blokland A (2005) Scopolamine-induced deficits in cognitive performance: a review of animal studies. Scopolamine Rev 1:1–76
2. Konar A, Shah N, Singh R, Saxena N, Kaul SC, Wadhwa R, Thakur MK (2011) Protective role of ashwagandha leaf extract and its component withanone on scopolamine-induced changes in the brain and brain-derived cells. PLoS One 6(11):e27265
3. Gautam A, Wadhwa R, Thakur MK (2013) Involvement of hippocampal arc in amnesia and its recovery by alcoholic extract of ashwagandha leaves. Neurobiol Learn Mem 106:177–184
4. Baghel MS, Thakur MK (2017) Differential proteome profiling in the hippocampus of amnesic mice. Hippocampus 27:845–859
5. Weeber EJ, Levy M, Sampson MJ, Anflous K, Armstrong DL, Brown SE, Sweatt JD, Craigen WJ (2002) The role of mitochondrial porins and the permeability transition pore in learning and synaptic plasticity. J Biol Chem 277:18891–18897
6. Huang H, Shah K, Bradbury NA, Li C, White C (2014) Mcl-1 promotes lung cancer cell migration by directly interacting with Vdac to increase mitochondrial Ca^{2+} uptake and reactive oxygen species generation. Cell Death Dis 5:e1482
7. Okada SF, O'Neal WK, Huang P, Nicholas RA, Ostrowski LE, Craigen WJ, Lazarowski ER, Boucher RC (2004) Voltage-dependent anion channel-1 (VDAC-1) contributes to ATP release and cell volume regulation in murine cells. J Gen Physiol 124:513–526
8. Kapogiannis D, Mattson MP (2011) Disrupted energy metabolism and neuronal circuit dysfunction in cognitive impairment and Alzheimer's disease. Lancet Neurol 10:187–198
9. Pathak D, Shields LY, Mendelsohn BA, Haddad D, Lin W, Gerencser AA, Kim H, Brand MD et al (2015) The role of mitochondrially derived ATP in synaptic vesicle recycling. J Biol Chem 290:22325–22236
10. Marsicano G, Lafenêtre P (2009) Roles of the endocannabinoid system in learning and memory. Curr Top Behav Neurosci 1:201–230
11. Broyd SJ, van Hell HH, Beale C, Yücel M, Solowij N (2016) Acute and chronic effects of cannabinoids on human cognition—a systematic review. Biol Psychiatry 79:557–567
12. Hebert-Chatelain E, Desprez T, Serrat R, Bellocchio L, Soria-Gomez E, Busquets-Garcia A, Pagano Zottola AC, Delamarre A et al (2016) A cannabinoid link between mitochondria and memory. Nature 539:555–559
13. Hagihara H, Toyama K, Yamasaki N, Miyakawa T (2009) Dissection of hippocampal dentate gyrus from adult mouse. J Vis Exp 17. https://doi.org/10.3791/1543
14. Ji XF, Chi TY, Xu Q, He XL, Zhou XY, Zhang R, Zou LB (2014) Xanthoceraside ameliorates mitochondrial dysfunction contributing to the improvement of learning and memory impairment in mice with intracerebroventricular injection of aβ1–42. Evid Based Complement Alternat Med 2014:969342
15. Premkumar A, Simantov R (2002) Mitochondrial voltage-dependent anion channel is involved in dopamine-induced apoptosis. J Neurochem 82:345–352
16. Prins JM, Park S, Lurie D (2010) Decreased expression of the voltage-dependent anion channel in differentiated PC-12 and SH-SY5Y cells following low-level Pb exposure. Toxicol Sci 113:169–176
17. Bradford MM (1976) A rapid and sensitive method for the quantitation of microgram quantities of protein utilizing the principle of protein-dye binding. Anal Biochem 72:248–254
18. Chida J, Yamane K, Takei T, Kido H (2012) An efficient extraction method for quantitation of adenosine triphosphate in mammalian tissues and cells. Anal Chim Acta 727:8–12
19. Paramanik V, Thakur MK (2012) Estrogen receptor β and its domains interact with casein kinase 2, phosphokinase C, and N-myristoylation sites of mitochondrial and nuclear proteins in mouse brain. J Biol Chem 287:22305–22316
20. Jain K, Prasad D, Singh SB, Kohli E (2015) Hypobaric hypoxia imbalances mitochondrial dynamics in rat brain hippocampus. Neurol Res Int 2015:742059

21. Saetersdal T, Engedal H, Røli J, Myklebust R (1980) Calcium and magnesium levels in isolated mitochondria from human cardiac biopsies. Histochemistry 68:1–8
22. Mishra VK, Upadhyay AR, Pandey SK, Tripathi BD (2008) Concentrations of heavy metals and aquatic macrophytes of Govind Ballabh Pant Sagar an anthropogenic lake affected by coal mining effluent. Environ Monit Assess 141:49–58
23. Das L, Vinayak M (2014) Long term effect of curcumin in regulation of glycolytic pathway and angiogenesis via modulation of stress activated genes in prevention of cancer. PLoS One 9:e99583
24. Weydert CJ, Cullen JJ (2010) Measurement of superoxide dismutase, catalase and glutathione peroxidase in cultured cells and tissue. Nat Protoc 5:51–66
25. Qiu JH, Asai A, Chi S, Saito N, Hamada H, Kirino T (2000) Proteasome inhibitors induce cytochrome c-caspase-3-like protease-mediated apoptosis in cultured cortical neurons. J Neurosci 20:259–265
26. Schmued LC, Stowers CC, Scallet AC, Xu L (2005) Fluoro-Jade C results in ultra high resolution and contrast labeling of degenerating neurons. Brain Res 1035:24–31
27. Ehara A, Ueda S (2009) Application of Fluoro-Jade C in acute and chronic neurodegeneration models: utilities and staining differences. Acta Histochem Cytochem 42:171–179
28. Klein AM, Ferrante RJ (2007) The neuroprotective role of creatine. Creatine and creatine kinase in health and disease. Springer, Berlin, pp 205–243
29. Huizing M, DePinto V, Ruitenbeek W, Trijbels FJ, van den Heuvel LP, Wendel U (1996) Importance of mitochondrial transmembrane processes in human mitochondriopathies. J Bioenerg Biomembr 28:109–114
30. Anflous K, Armstrong DD, Craigen WJ (2001) Altered mitochondrial sensitivity for ADP and maintenance of creatine-stimulated respiration in oxidative striated muscles from VDAC1-deficient mice. J Biol Chem 276:1954–1960
31. Anflous-Pharayra K, Lee N, Armstrong DL, Craigen WJ (2011) VDAC3 has differing mitochondrial functions in two types of striated muscles. Biochim Biophys Acta 1807:150–156
32. Loubiere C, Clavel S, Gilleron J, Harisseh R, Fauconnier J, Ben-Sahra I, Kaminski L, Laurent K et al (2017) The energy disruptor metformin targets mitochondrial integrity via modification of calcium flux in cancer cells. Sci Rep 7:5040
33. Carvalho C, Correia SC, Cardoso S, Plácido AI, Candeias E, Duarte AI, Moreira PI (2015) The role of mitochondrial disturbances in Alzheimer, Parkinson and Huntington diseases. Expert Rev Neurother 15:867–884
34. Sheridan C, Martin SJ (2010) Mitochondrial fission/fusion dynamics and apoptosis. Mitochondrion 10:640–648
35. Chinopoulos C, Adam-Vizi V (2010) Mitochondrial Ca2+ sequestration and precipitation revisited. FEBS J 277:3637–3651
36. Carafoli E (2010) The fateful encounter of mitochondria with calcium: how did it happen? Biochim Biophys Acta 1797:595–606
37. Pivovarova NB, Nguyen HV, Winters CA, Brantner CA, Smith CL, Andrews SB (2004) Excitotoxic calcium overload in a subpopulation of mitochondria triggers delayed death in hippocampal neurons. J Neurosci 24:5611–5622
38. Wang CH, Wu SB, Wu YT, Wei YH (2013) Oxidative stress response elicited by mitochondrial dysfunction: implication in the pathophysiology of aging. Exp Biol Med 238:450–460
39. Guo JY, Xia B, White E (2013) Autophagy-mediated tumor promotion. Cell 155:1216–1219
40. Maharjan S, Oku M, Tsuda M, Hoseki J, Sakai Y (2014) Mitochondrial impairment triggers cytosolic oxidative stress and cell death following proteasome inhibition. Sci Rep 4:5896
41. Vander Heiden MG, Chandel NS, Williamson EK, Schumacker PT, Thompson CB (1997) Bcl-xL regulates the membrane potential and volume homeostasis of mitochondria. Cell 91:627–637
42. Narita M, Shimizu S, Ito T, Chittenden T, Lutz RJ, Matsuda H, Tsujimoto Y (1998) Bax interacts with the permeability transition pore to induce permeability transition and cytochrome c release in isolated mitochondria. Proc Natl Acad Sci U S A 95:14681–14686
43. Arbel N, Ben-Hail D, Shoshan-Barmatz V (2012) Mediation of the antiapoptotic activity of Bcl-xL protein upon interaction with VDAC1 protein. J Biol Chem 287:23152–23161
44. Arif T, Vasilkovsky L, Refaely Y, Konson A, Shoshan-Barmatz V (2014) Silencing VDAC1 expression by siRNA inhibits cancer cell proliferation and tumor growth in vivo. Mol Ther Nucleic Acids 3: e159
45. Dubey AK, Godbole A, Mathew MK (2016) Regulation of VDAC trafficking modulates cell death. Cell Death Discov 2:16085